

Structure determination of multilayer silicene grown on Ag(111) films by electron diffraction: Evidence for Ag segregation at the surface

Terufusa Shirai,¹ Tetsuroh Shirasawa,^{2,3} Toru Hirahara,^{1,*} Naoya Fukui,¹ Toshio Takahashi,² and Shuji Hasegawa¹

¹*Department of Physics, University of Tokyo, 7-3-1 Hongo, Bunkyo-ku, Tokyo 113-0033, Japan*

²*Institute for Solid State Physics, University of Tokyo, 5-1-5 Kashiwanoha, Kashiwa 277-8581, Japan*

³*JST, PRESTO, 4-1-8 Honcho Kawaguchi, Saitama, Japan*

(Received 2 May 2014; revised manuscript received 28 May 2014; published 10 June 2014)

The structure of multilayer silicene formed on Ag(111) films was studied by low-energy electron diffraction. It turned out that the experimental data cannot be explained by proposed models that only consider buckling of silicon atoms. We have rather found that multilayer silicene on Ag(111) is actually a thin film of bulklike silicon terminated with the Si(111) $\sqrt{3} \times \sqrt{3}$ -Ag surface. The results are compared to previous works and clearly show the importance to properly understand the structure of the system when discussing its electronic properties.

DOI: [10.1103/PhysRevB.89.241403](https://doi.org/10.1103/PhysRevB.89.241403)

PACS number(s): 68.35.-p, 61.05.J-, 73.20.-r

Silicene is a monolayer sheet of silicon and believed to host Dirac electrons similar to graphene [1,2]. Experimental studies have been extensively performed recently to reveal the presence of the Dirac-cone-type bands and associated intriguing properties [3–19]. For example, it was shown that silicene can be formed when making ZrB₂ on Si(111). Unfortunately, the electronic properties of the system were different from the freestanding silicene and no clear evidence of Dirac-cone features was found [3,4]. This was explained as due to the strong interaction with the substrate. The most frequently used substrate is Ag(111), and angle-resolved photoemission spectroscopy (ARPES) measurements showed the presence of linearly dispersing states near E_F for monolayer silicene [3×3 superstructure with respect to the Si(111) lattice] [7]. However, it was shown that this state also consists of Ag orbitals [20,21], thus implying that the Dirac-cone character is lost due to the interaction of Si with Ag. This was also confirmed with structure analysis [16,17], and also pointed out for Si nanoribbons on Ag(110) [22].

One idea to get around this problem of the substrate-silicene interaction is to deposit Si further and make multilayer silicene; the second-layer silicene would weakly interact with the first-layer silicene. The $\sqrt{3} \times \sqrt{3}$ structure on Ag(111) was verified as multilayer silicene [10,18], although some claimed it was still a single layer [12]. Several structure models have been proposed [12,23,24]. There is also a debate about the presence or absence of Dirac fermions in this system. Chen *et al.* reported from scanning tunneling microscopy (STM) and scanning tunneling spectroscopy (STS) measurements that the carriers in this system had a linear dispersion [12,24,25], while Arafune *et al.* claimed that the dispersion was parabolic using the same method [18]. ARPES measurements also showed the existence of metallic carriers and assigned it as a Dirac fermion [10,11]. However, the Fermi velocities of the two measurements were not consistent with each other (1.2×10^6 m/s for STM/STS [12], 3.5×10^5 m/s for ARPES [10]). Furthermore, it was also reported that this system can show superconductivity [26] or some spontaneous symmetry breaking [24]. As such, there are

still many things that need to be clarified to fully understand the intriguing properties of multilayer silicene.

Therefore in the present study, we have performed structural analysis on this multilayer silicene formed on Ag(111) with low-energy electron diffraction (LEED). We found that the proposed models for multilayer silicene cannot explain the experimental data. Instead, it was well analyzed by assuming a thin film of diamondlike silicon with the Si(111) $\sqrt{3} \times \sqrt{3}$ -Ag structure at the surface. Moreover, our results can explain the parabolic and linear band dispersions reported in Refs. [12,19,24,25] and the phase transition to a lower symmetric structure (Ref. [24]). However, it is still not possible to understand all the previous experimental works and probably calls for a precise fine tuning of the silicene growth condition.

All the sample fabrication was done *in situ* under reflection high-energy electron diffraction (RHEED) observations. First, a clean Si(111)- 7×7 surface was prepared on an *n*-type substrate (P-doped, 1–10 Ω cm at room temperature) by a cycle of resistive heat treatments. Then Ag was deposited at room temperature to grow the Ag(111) film. The film thickness was 20 ML_{Ag} (1 ML_{Ag} = 1.39×10^{15} atoms/cm², 2.36 Å thick). Then Si was deposited on the Ag film at 500 K to produce silicene [7]. We deposited ~ 4 ML_{Si} of Si (1 ML_{Si} = 7.84×10^{14} atoms/cm², 3.13 Å thick) which was approximately calibrated by the formation of the single-layer 3×3 phase.

The surface structure analysis was performed with the LEED intensity vs voltage (IV) analysis. IV curves were obtained at 100 K. The LEED patterns with incident energy from 80 to 300 eV were recorded in steps of 1 eV by a digital CCD camera. In order to determine the atomic structure, we calculated the IV curves in the tensor LEED to fit the experimental IV curves using the SATLEED package of Barbieri *et al.* [27]. The in-plane lattice constant was determined from positions of the LEED spots. Angular momentum up to 14 ($l_{\max} = 14$) was taken into account. In search of the optimal structure that had the minimum Pendry's R factor (R_p), the Debye temperature of each atom was changed in steps of 10 K.

Figures 1(a) and 1(b) show the RHEED (a) and LEED (b) patterns of the 20 ML_{Ag} Ag(111) film, respectively, showing the 1×1 periodicity in terms of the Ag lattice constant. The RHEED patterns were taken with an incident energy of 15 keV

*Present address: Department of Physics, Tokyo Institute of Technology, 2-12-1 Ookayama, Meguro-ku, Tokyo 152-8551, Japan; hirahara@phys.titech.ac.jp

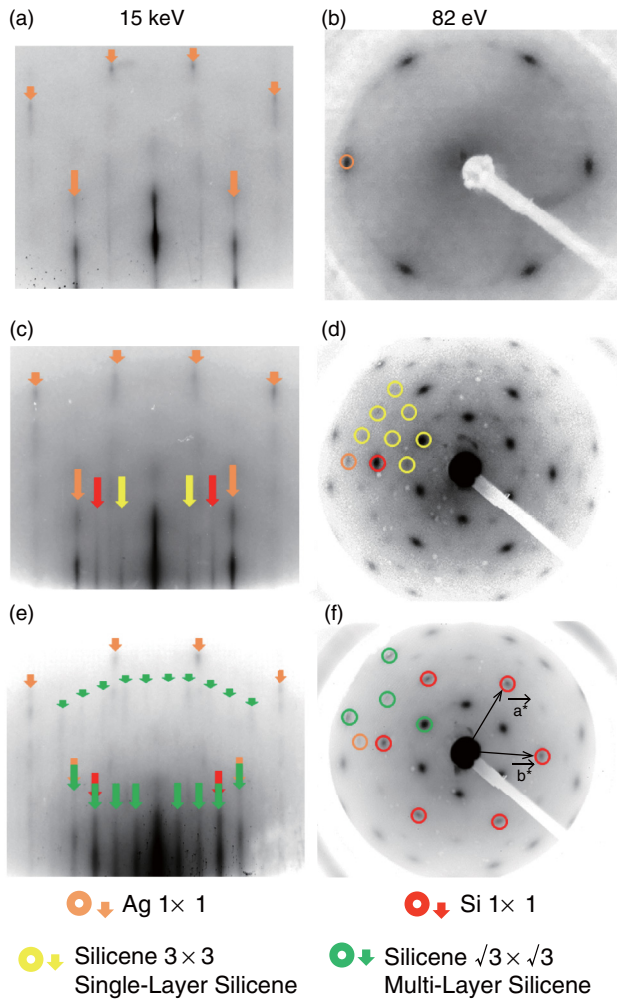


FIG. 1. (Color online) RHEED and LEED patterns for Ag(111)- 1×1 [(a) and (b)], single-layer silicene (3×3) [(c) and (d)], and multilayer ($\sim 4 \text{ ML}_{\text{Si}}$) silicene ($\sqrt{3} \times \sqrt{3}$) [(e) and (f)], respectively. The RHEED (LEED) patterns were taken at room temperature (100 K). The incident electron energy is 15 keV, and 82 eV, respectively.

throughout this Rapid Communication. The LEED patterns shown in Fig. 1 were taken at 82 eV. After Si deposition at 500 K, additional spots appear, as shown in Figs. 1(c) and 1(d). Red arrows or circles correspond to spots for the Si 1×1 periodicity. The yellow circles in the LEED pattern of Fig. 1(d) correspond to the 3×3 (or 4×4 in terms of the Ag lattice) spots that have been identified as the signature of the completion of the first Si layer on Ag(111) [7,18]. However in the RHEED pattern of Fig. 1(c), there is no clear 3×3 periodicity, and only some additional spots at the zeroth Laue zone (yellow arrows) appear. This may be due to the fact that the sample was cooled down in the LEED measurements to 100 K, while the RHEED observation was done at room temperature (Debye-Waller effect). Since the yellow arrow spots were observed every time the silicene sample was fabricated, we regard this as the signature of the completion of the single-layer silicene on Ag(111). After further deposition of Si, namely, about twice the amount of deposition time as that shown in Figs. 1(c) and 1(d), clear $\sqrt{3} \times \sqrt{3}$ spots

appear as can be seen in Figs. 1(e) and 1(f) (green arrows and circles). Even the first Laue zone of the Si(111) periodicity can be observed in Fig. 1(e) (short green arrows), and the 1×1 spots of the Ag(111) lattice become weak (orange arrows and circles). This is consistent with previous reports and can be regarded as the formation of multilayer silicene [10,18]. We have also found that the $\sqrt{3} \times \sqrt{3}$ is preserved even when Si is further deposited and the Si thickness for the sample shown in Figs. 1(e) and 1(f) is 4 ML_{Si} . We will call it “M-silicene” hereafter.

The red curves in Figs. 2(a) and 2(b) show the experimentally determined LEED IV curves for the M-silicene sample shown in Figs. 1(e) and 1(f). Eight different spots in the LEED pattern have been plotted. Despite the threefold symmetry of the $\sqrt{3} \times \sqrt{3}$ structure, the symmetrically inequivalent spots, such as $(1\ 0)$ and $(0\ 1)$ spots, exhibited almost the same IV curves. This is because there are twin domains on the surface, which are mirror reflected to each other, and thus their superposition leads to the apparent twofold symmetry. Taking this double-domain surface into account, we took the average of the IV curves both in the calculation and in the experimental data such that $\{hk\}$ is the average of the two double-domain symmetric points (hk) and (kh) . Note that some spots such as $(2/3\ 2/3)$ do not need averaging. The details concerning the symmetry will be discussed further later in Fig. 3.

Now let us move on to the analysis of the experimental data. As a starting point for the analysis, we have adopted structure models that have been proposed in the literature [12,23,24]. They are basically multilayer buckled silicene structures stacked in different sequences [12]. The substrate Ag atoms are considered in some models [23,24]. We have varied the amount of buckling (0.05–0.8 Å) and the interlayer distances between the layers (1.0–3.0 Å) considering the height difference reported in STM studies [9,15]. Four topmost buckled Si layers were allowed to relax. However, we were not able to reproduce the experimental data for any of the proposed models (R_p was 0.6–0.8).

Therefore, we reached the conclusion that it is likely that the M-silicene we experimentally fabricated is not only composed of Si. In fact, we realized that the experimental curves of Figs. 2(a) and 2(b) are similar to those of the Si(111)- $\sqrt{3} \times \sqrt{3}$ -Ag surface reported in Refs. [28] and [29]. Hence we have adopted the honeycomb-chain triangle (HCT) [Fig. 2(c)] [30] and inequivalent triangle (IET) models [Fig. 2(d)] [31] as the initial structure and performed the LEED IV analysis [32]. The topmost Ag layer as well as the four Si bilayers below were allowed to relax and below it, the parameters for the diamondlike Si(111) bilayers (buckling = 0.78 Å and interlayer distance = 2.35 Å) were used [Fig. 2(e)] [33]. The comparison between experiment and calculation is shown in Figs. 2(a) and 2(b), which show nice agreement [$R_p = 0.22 \pm 0.03$ in (a) and $R_p = 0.19 \pm 0.03$ in (b)]. The optimized structure is shown in Fig. 2(e), and we can say that the structure is close to a diamondlike silicon terminated with $\sqrt{3} \times \sqrt{3}$ -Ag structure at the surface. The Debye temperature and other parameters are also shown in Fig. 2(e), and they are close to those reported in Refs. [28–30].

Our analysis above suggests that M-silicene is basically a diamond-lattice silicon film with Si(111)- $\sqrt{3} \times \sqrt{3}$ -Ag at the surface. However one needs to be careful before reaching

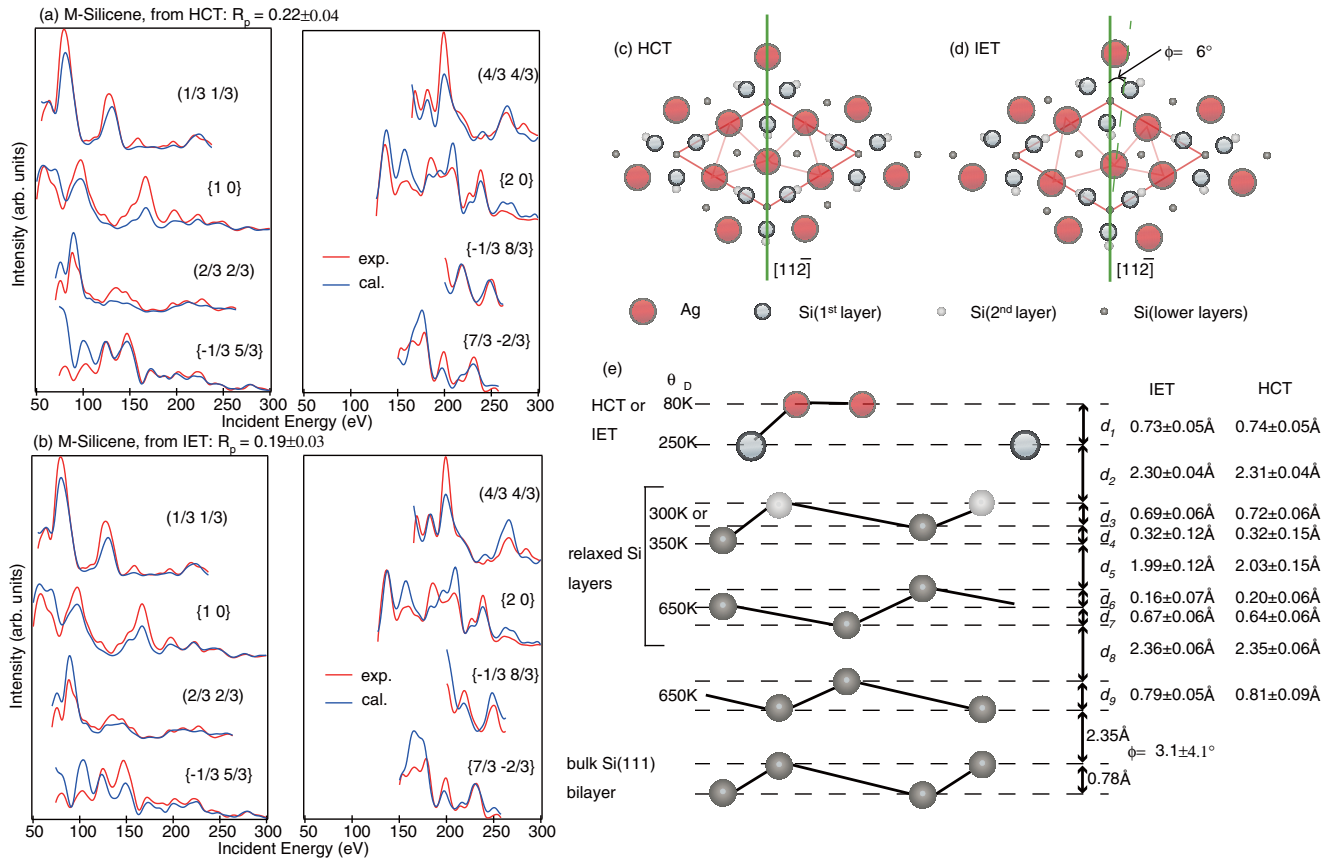


FIG. 2. (Color online) (a), (b) Experimentally measured and calculated LEED IV curves for the multilayer silicene $\sqrt{3} \times \sqrt{3}$ structure at 100 K for various spots. The HCT model (c) is the starting structure for the analysis in (a), and the IET model (d) for the analysis in (b). (e) The side view of the optimized structure with various parameters.

a final conclusion; since we made silicene on the Ag(111) film on the Si(111) substrate, it may just be that we have annealed the Ag(111) film at too high temperature during Si deposition and it broke the Ag(111) film to form the

Si(111) $\sqrt{3} \times \sqrt{3}$ -Ag structure. To examine this possibility, we deposited 1 ML_{Si} of Ag on the Si(111)-7 × 7 substrate at 650 K to form the Si(111) $\sqrt{3} \times \sqrt{3}$ -Ag surface, and measured its LEED IV curve. It is shown in Fig. 3(a) together with that of M-silicene [34]. The actual LEED pattern at 79 eV is shown in Fig. 3(c). Compared to that of M-silicene [Fig. 3(b)], the spots for $\sqrt{3} \times \sqrt{3}$ -Ag are much sharper with high signal-to-noise ratio. Furthermore, there is a difference in symmetry; the $\sqrt{3} \times \sqrt{3}$ -Ag has threefold symmetry as indicated by the boxes and circles, while M-silicene is sixfold symmetric. This can actually be seen in the IV curves of Fig. 3(a). While the basic shapes are similar between the two structures, the IV curves for the $\sqrt{3} \times \sqrt{3}$ -Ag surface show a clear difference among the two inequivalent spots, e.g., (5/3 -1/3) and (-1/3 5/3). This symmetry difference originates from the presence of a mirror-reflected domain. For the Si(111) $\sqrt{3} \times \sqrt{3}$ -Ag surface, the threefold symmetry is due to the threefold symmetry of bulk silicon. On the other hand, since M-silicene is epitaxially grown on Ag(111) film which also shows a sixfold symmetry [Fig. 1(b)], there is a freedom to form a twin domain structure. Thus we conclude that the sample for which we measured the LEED IV curve of Fig. 2 is not the Si(111) $\sqrt{3} \times \sqrt{3}$ -Ag surface that was formed directly on the Si(111) substrate by breaking the Ag(111) film. This is also supported by photoemission measurements where they found that the Ag(111) film does not break until annealing up to 600 K [35].

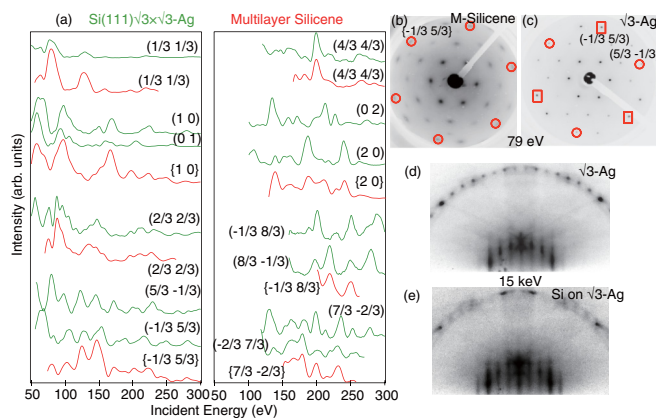


FIG. 3. (Color online) (a) Comparison of the experimental LEED IV curves for the Si(111) $\sqrt{3} \times \sqrt{3}$ -Ag surface and multilayer silicene. (b), (c) LEED patterns taken at 79 eV for Si(111) $\sqrt{3} \times \sqrt{3}$ -Ag (b) and multilayer silicene (c), respectively. A threefold symmetry can be observed in (b) while a sixfold symmetry can be seen in (c) due to the twin domains. (d), (e) RHEED patterns of pristine Si(111) $\sqrt{3} \times \sqrt{3}$ -Ag (d) and 4 ML_{Si} Si deposited on Si(111) $\sqrt{3} \times \sqrt{3}$ -Ag (e), respectively.

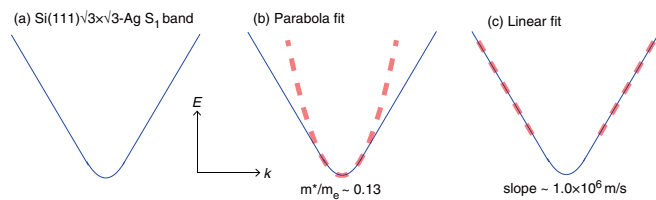


FIG. 4. (Color online) (a) Schematic drawing of the dispersion of the S_1 band of the $\text{Si}(111)\sqrt{3} \times \sqrt{3}$ -Ag surface taken from Ref. [31]. It can be fitted with a parabola at the bottom as shown in (b), and with a line away from the bottom as shown in (c).

Finally, we have performed an additional RHEED observation to see the stability of the $\sqrt{3} \times \sqrt{3}$ -Ag surface termination. As mentioned in the introduction, the $\sqrt{3} \times \sqrt{3}$ pattern is maintained after 2 ML_{Si} of Si deposition on the Ag(111) surface. Our analysis showed that this is actually close to the diamond Si structure with $\text{Si}(111)\sqrt{3} \times \sqrt{3}$ -Ag at the topmost layers. Therefore it indicates that the deposited Si atoms are incorporated into the underlying layers to form the diamond structure and the surface made of Ag and Si is preserved. Figure 3(d) shows the RHEED pattern of the pristine $\text{Si}(111)\sqrt{3} \times \sqrt{3}$ -Ag surface and Fig. 3(e) shows the RHEED pattern after deposition of $\sim 4 \text{ ML}_{\text{Si}}$ of Si on top of it at 500 K. This condition is the same as when M-silicene is formed on the Ag(111) film. It can be clearly seen that the $\sqrt{3} \times \sqrt{3}$ periodicity is maintained during and after deposition. This indicates that the $\text{Si}(111)\sqrt{3} \times \sqrt{3}$ -Ag surface is energetically more favorable than forming other structures, and is consistent with the fact the multilayer silicene always shows the $\sqrt{3} \times \sqrt{3}$ surface periodicity. It means that Ag acts as a surfactant in the Si growth process. Similar surfactant behavior has been found for the Ag growth on Bi/Ag(111) [36] or Ge growth on Bi/Si(111) surfaces [37].

Now let us discuss the present findings in comparison with the results shown in previous studies. First, we discuss the phase transition for M-silicene. As mentioned, it has been reported that M-silicene undergoes a spontaneous symmetry breaking by forming twin domains of a $p3$ symmetry structure below 40 K [19,24]. It is well known that the $\text{Si}(111)\sqrt{3} \times \sqrt{3}$ -Ag surface also shows this kind of transition. Namely, the IET structures ($p3$ symmetry) which are characterized by $\pm 6^\circ$ rotation of the Ag triangles with respect to the HCT structure ($p31m$), fluctuate above $T_c = 120$ K and show the honeycomb structure in the STM images. Below T_c , the fluctuation stops and the STM image becomes a hexagonal lattice [38]. Although the transition temperature is different, the STM images for M-silicene and $\text{Si}(111)\sqrt{3} \times \sqrt{3}$ -Ag are similar to each other and we suspect that this is basically the freeze of the fluctuation between the two IET structures. The decrease of T_c for M-silicene may be related to the presence of twin domains, or a finite size effect [39] due to the smaller

domain size of the $\sqrt{3} \times \sqrt{3}$ structure which can be seen from the broader LEED spots [Figs. 3(b) and 3(c)].

The debate of the presence or absence of the Dirac cone can be partially explained as follows. For the $\text{Si}(111)\sqrt{3} \times \sqrt{3}$ -Ag surface, it is well known that a metallic surface state exists, the so-called S_1 state. Its dispersion is shown schematically in Fig. 4(a), adapted from the first-principles calculation of Ref. [31]. Near the bottom of the band, it is free-electron-like [Fig. 4(b)] and the effective mass of the parabola has been determined with ARPES and STM and STS measurements to be $(0.13 \pm 0.03)m_e$ (m_e is the mass of free electrons) [40]. Reference [19] reported that the band dispersion of the carriers in M-silicene is parabolic with an effective mass of $0.14m_e$ from the quasiparticle interference patterns of STM and STS measurements. Moreover, Chen *et al.* have shown that the dispersion is linear when the energy increases with a Fermi velocity of 1.2×10^6 m/s. This is close to the linear slope of the S_1 state obtained in Ref. [31] [1.0×10^6 m/s, Fig. 4(c)]. Therefore, it is likely that the samples they fabricated were similar to ours and the $\text{Si}(111)\sqrt{3} \times \sqrt{3}$ -Ag surface was formed on the topmost layers.

However, we still cannot explain the band dispersion data obtained by ARPES [10,11]. Even if the metallic band in the ARPES image of Ref. [10] was fitted with a parabola, the effective mass would be larger than 0.13 (~ 0.59) and cannot be the S_1 band of the $\text{Si}(111)\sqrt{3} \times \sqrt{3}$ -Ag surface. Thus it may be possible that there is a narrow window in which one can fabricate M-silicene without Ag surface segregation. If the temperature is not at this optimum condition, the $\text{Si}(111)\sqrt{3} \times \sqrt{3}$ -Ag structure is formed at the surface and the intriguing intrinsic properties of silicene may be hindered. Considering the complex phase diagram of the silicene fabrication condition on Ag(111) [18], a fine tuning of the substrate temperature during Si deposition (and also the deposition rate) should be necessary to fabricate silicene.

In conclusion, we have performed LEED IV measurements and determined the atomic structure for multilayer silicene on Ag(111). It turned out that M-silicene is a thin film of diamond silicon and terminated with the $\text{Si}(111)\sqrt{3} \times \sqrt{3}$ -Ag surface. The present result is partially consistent with previous experimental works, but not with others. Our results strongly recall the importance to understand the atomic structure properly in discussing the electronic property of low-dimensional systems. Further experimental work is needed to explore the ideal conditions in which to fabricate silicene and explore its predicted intriguing properties.

The present work has been supported by Grants-in-Aid for Scientific Research Program (Grants No. 25246025 and No. 25600093) from the Japan Society for the Promotion of Science and that in New Academic Field “Molecular Architectonics” (Grant No. 25110010) by the Ministry of Education, Culture, Sports, Science and Technology.

[1] K. Takeda and K. Shiraishi, *Phys. Rev. B* **50**, 14916 (1994).
 [2] S. Cahangirov, M. Topsakal, E. Aktürk, H. Sahin, and S. Ciraci, *Phys. Rev. Lett.* **102**, 236804 (2009).

[3] A. Fleurence, R. Friedlein, T. Ozaki, H. Kawai, Y. Wang, and Y. Yamada-Takamura, *Phys. Rev. Lett.* **108**, 245501 (2012).

- [4] R. Friedlein, A. Fleurence, J. T. Sadowski, and Y. Yamada-Takamura, *Appl. Phys. Lett.* **102**, 221603 (2013).
- [5] L. Meng, Y. Wang, L. Zhang, S. Du, R. Wu, L. Li, Y. Zhang, G. Li, H. Zhou, W. A. Hofer, and H.-J. Gao, *Nano Lett.* **13**, 685 (2013).
- [6] M. Švec, P. Hapala, M. Ondráček, P. Merino, M. Blanco-Rey, P. Mutombo, M. Vondráček, Y. Polyak, V. Cháb, J. A. Martín Gago, and P. Jelínek, *Phys. Rev. B* **89**, 201412(R) (2014).
- [7] P. Vogt, P. De Padova, C. Quaresima, J. Avila, E. Frantzeskakis, M. C. Asensio, A. Resta, B. Ealet, and G. Le Lay, *Phys. Rev. Lett.* **108**, 155501 (2012).
- [8] J. Avila, P. De Padova, S. Cho, I. Colambo, S. Lorey, C. Quaresima, P. Vogt, A. Resta, G. Le Lay, and M. C. Asensio, *J. Phys.: Condens. Matter* **25**, 262001 (2013).
- [9] A. Resta, T. Leoni, C. Barth, A. Ranguis, C. Becker, T. Bruhn, P. Vogt, and G. Le Lay, *Sci. Rep.* **3**, 2399 (2013).
- [10] P. De Padova, P. Vogt, A. Resta, J. Avila, I. Razado-Colambo, C. Quaresima, C. Ottaviani, B. Olivieri, T. Bruhn, T. Hirahara, T. Shirai, S. Hasegawa, M. Carmen Asensio, and G. Le Lay, *Appl. Phys. Lett.* **102**, 163106 (2013).
- [11] P. De Padova, J. Avila, A. Resta, I. Razado-Colambo, C. Quaresima, C. Ottaviani, B. Olivieri, T. Bruhn, P. Vogt, M. C. Asensio, and G. Le Lay, *J. Phys.: Condens. Matter* **25**, 382202 (2013).
- [12] L. Chen, C.-C. Liu, B. Feng, X. He, P. Cheng, Z. Ding, S. Meng, Y. Yao, and K. Wu, *Phys. Rev. Lett.* **109**, 056804 (2012).
- [13] B. Feng, Z. Ding, S. Meng, Y. Yao, X. He, P. Cheng, L. Chen, and K. Wu, *Nano Lett.* **12**, 3507 (2012).
- [14] C.-L. Lin, R. Arafune, K. Kawahara, M. Kanno, N. Tsukahara, E. Minamitani, Y. Kim, M. Kawai, and N. Takagi, *Phys. Rev. Lett.* **110**, 076801 (2013).
- [15] C.-L. Lin, R. Arafune, K. Kawahara, N. Tsukahara, E. Minamitani, Y. Kim, N. Takagi, and M. Kawai, *Appl. Phys. Exp.* **5**, 045802 (2012).
- [16] K. Kawahara, T. Shirasawa, R. Arafune, C. L. Lin, T. Takahashi, M. Kawai, and N. Takagi, *Surf. Sci.* **623**, 25 (2014).
- [17] Y. Fukaya, I. Mochizuki, M. Maekawa, K. Wada, T. Hyodo, I. Matsuda, and A. Kawasuso, *Phys. Rev. B* **88**, 205413 (2013).
- [18] R. Arafune, C.-L. Lin, K. Kawahara, N. Tsukahara, E. Minamitani, Y. Kim, N. Takagi, and M. Kawai, *Surf. Sci.* **608**, 297 (2013).
- [19] R. Arafune, C. L. Lin, R. Nagao, M. Kawai, and N. Takagi, *Phys. Rev. Lett.* **110**, 229701 (2013).
- [20] Z.-X. Guo, S. Furuya, J. I. Iwata, and A. Oshiyama, *Phys. Rev. B* **87**, 235435 (2013).
- [21] S. Cahangirov, M. Audiffred, P. Tang, A. Iacomino, W. Duan, G. Merino, and A. Rubio, *Phys. Rev. B* **88**, 035432 (2013).
- [22] F. Ronci, G. Serrano, P. Gori, A. Cricenti, and S. Colonna, *Phys. Rev. B* **89**, 115437 (2014).
- [23] Z.-X. Guo and A. Oshiyama, *Phys. Rev. B* **89**, 155418 (2014).
- [24] L. Chen, H. Li, B. Feng, Z. Ding, J. Qiu, P. Cheng, K. Wu, and S. Meng, *Phys. Rev. Lett.* **110**, 085504 (2013).
- [25] L. Chen, C.-C. Liu, B. Feng, X. He, P. Cheng, Z. Ding, S. Meng, Y. Yao, and K. Wu, *Phys. Rev. Lett.* **110**, 229702 (2013).
- [26] L. Chen, B. Feng, and K. Wu, *Appl. Phys. Lett.* **102**, 081602 (2013).
- [27] M. A. Van Hove, W. Moritz, H. Over, P. J. Rous, A. Wander, A. Barbieri, N. Materer, and U. Starke, *Surf. Sci. Rep.* **19**, 191 (1993).
- [28] H. Over, H. Huang, S. Y. Tong, W. C. Fan, and A. Ignatiev, *Phys. Rev. B* **48**, 15353 (1993).
- [29] H. Over, S. Y. Tong, J. Quinn, and F. Jona, *Surf. Rev. Lett.* **2**, 451 (1995).
- [30] T. Takahashi and S. Nakatani, *Surf. Sci.* **282**, 17 (1993).
- [31] H. Aizawa, M. Tsukada, N. Sato, and S. Hasegawa, *Surf. Sci.* **429**, L509 (1999).
- [32] As mentioned below, M-silicene is reported to show a phase transition below $T_c = 40$ K which is likely related to symmetry lowering between the HCT and IET structures. Since our measurement temperature is 100 K (higher than T_c), we have done the analysis for both the HCT and IET structures. It suggests the difficulty to distinguish the two from the present measurement.
- [33] Since the $\text{Ag } 1 \times 1$ spots were very weak in Fig. 1(f), we have neglected the underlying $\text{Ag}(111)$ structure in the analysis.
- [34] See Supplemental Material at <http://link.aps.org/supplemental/10.1103/PhysRevB.89.241403> for the analysis of the LEED I V curves for the $\text{Si}(111)\sqrt{3} \times \sqrt{3}$ -Ag surface.
- [35] I. Matsuda, H. W. Yeom, T. Tanikawa, K. Tono, T. Nagao, S. Hasegawa, and T. Ohta, *Phys. Rev. B* **63**, 125325 (2001).
- [36] H. Fukumoto, M. Miyazaki, Y. Aoki, K. Nakatsuji, and H. Hirayama, *Surf. Sci.* **611**, 49 (2013).
- [37] J. Mysliveček, F. Dvůrák, A. Stróżecka, and B. Voigtländer, *Phys. Rev. B* **81**, 245427 (2010).
- [38] N. Sato, T. Nagao, and S. Hasegawa, *Surf. Sci.* **442**, 65 (1999).
- [39] H. Dosch, *Critical Phenomena at Surfaces and Interfaces* (Springer-Verlag, Berlin, 1992).
- [40] T. Hirahara, I. Matsuda, M. Ueno, and S. Hasegawa, *Surf. Sci.* **563**, 191 (2004).